● **RESEARCH ARTICLE**

Rab27a/Slp2-a complex is involved in Schwann cell myelination

Wen-feng Su[1], Yun Gu[1], Zhong-ya Wei[1], Yun-tian Shen[1], Zi-han Jin[1], Ying Yuan[1,2], Xiao-song Gu[1], Gang Chen[1,*]
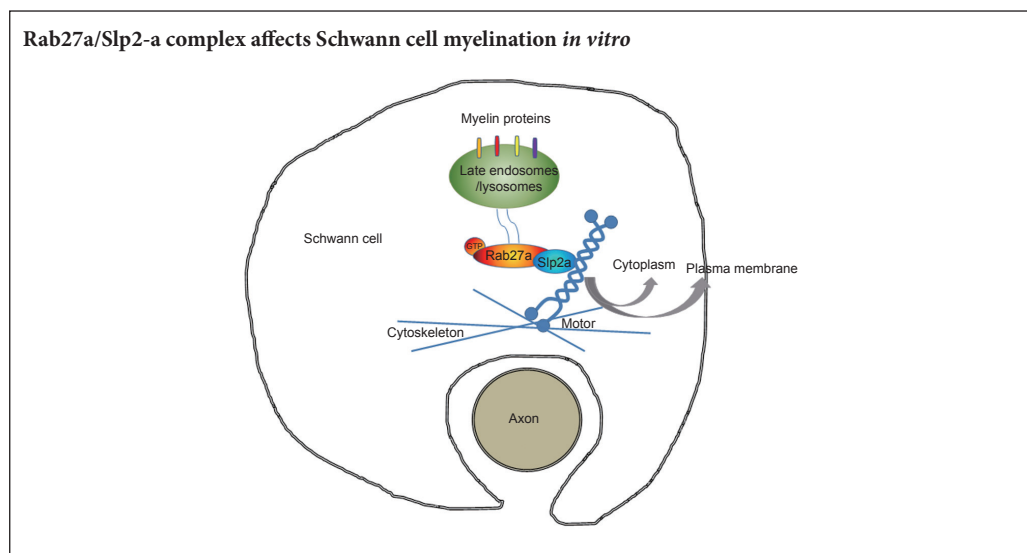
1 Jiangsu Key Laboratory of Neuroregeneration, Co-innovation Center of Neuroregeneration, Nantong University, Nantong, Jiangsu Province, China
2 Affiliated Hospital of Nantong University, Nantong, Jiangsu Province, China

Graphical Abstract

Rab27a/Slp2-a complex affects Schwann cell myelination *in vitro*

Correspondence to:
Gang Chen, Ph.D., M.D.,
chengang6626@ntu.edu.cn.

orcid:
0000-0003-3669-5687
(Gang Chen)

Abstract

Myelination of Schwann cells in the peripheral nervous system is an intricate process involving myelin protein trafficking. Recently, the role and mechanism of the endosomal/lysosomal system in myelin formation were emphasized. Our previous results demonstrated that a small GTPase Rab27a regulates lysosomal exocytosis and myelin protein trafficking in Schwann cells. In this present study, we established a dorsal root ganglion (DRG) neuron and Schwann cell co-culture model to identify the signals associated with Rab27a during myelination. First, Slp2-a, as the Rab27a effector, was endogenously expressed in Schwann cells. Second, Rab27a expression significantly increased during Schwann cell myelination. Finally, Rab27a and Slp2-a silencing in Schwann cells not only reduced myelin protein expression, but also impaired formation of myelin-like membranes in DRG neuron and Schwann cell co-cultures. Our findings suggest that the Rab27a/Slp2-a complex affects Schwann cell myelination *in vitro*.

Key Words: nerve regeneration; Schwann cells; dorsal root ganglion neurons; co-culture; myelin proteins; myelination; Rab27 effectors; Rab27a; Slp2-a; neural regeneration

Introduction

The myelin sheath in the peripheral nervous system (PNS) comprises a specialized Schwann cell plasma membrane, which serves to increase axonal impulse conduction (da Silva et al., 2014; Luo et al., 2014; Nave and Werner, 2014; Miyamoto et al., 2016; Taveggia, 2016). Clinically, abnormal myelination is a feature of many peripheral neuropathies that can cause abnormal electrical signal conduction and lead to secondary axonal injury (Duncan et al., 2014; Gonzalez et al., 2016; Klein and Martini, 2016; Kondo and Duncan, 2016; Schulz et al., 2016). The proper synthesis and transport of myelin proteins is important for myelin biogenesis (Kwon et al., 2013; Heller et al., 2014; Montani et al., 2014; Domènech-Estévez et al., 2015; Gökbuget et al., 2015).

However, the mechanisms regulating myelin protein trafficking remain poorly understood (White and Krämer-Albers, 2014; Salzer, 2015; Ma et al., 2016; Rao and Pearse, 2016).

Recently, the role and mechanisms of the endosomal/lysosomal system in myelin formation were investigated (Trajkovic et al., 2006; Prolo et al., 2009; Feldmann et al., 2011; Shen et al., 2016). Neuronal signals induce exocytose is of the proteolipid protein (PLP) from late endosome/lysosome membranes stored into the plasma membrane (Trajkovic et al., 2006; Shen et al., 2016). Consistent with this finding, myelin abnormalities are a very common phenomenon in many lysosomal storage diseases, including multiple sulfatase deficiency, globoid cell leukodystrophy, and metachromatic leukodystrophy (Faust et al., 2010; Marsden and Levy, 2010). Because lysosomes serve dual functions in many cell types–the degradation of proteins and storage of synthesized secretory products (Blott and Griffiths, 2002; de Duve, 2005; Zhang et al., 2007; Johnson et al., 2013; Kim et al., 2013; Hou et al., 2015; Shimada-Sugawara et al., 2015)–the concept of secretory lysosomes was proposed.

Previous studies have shown that the Rab27 subfamily and their multiple effectors play a critical role in regulating lysosome-related organelle exocytosis (Izumi, 2007; Johnson et al., 2013; Shimada-Sugawara et al., 2015; Yamaoka et al., 2015b, a). Additionally, our previous results showed that Rab27a participates in lysosomal exocytosis and myelin protein P0 trafficking in Schwann cells. Furthermore, Rab27a-deficient ashen mice demonstrate impaired demyelination of the injured sciatic nerve (Chen et al., 2012). In this study, we further investigated the mechanisms of Rab27a in the regulation of Schwann cell myelination by the dorsal root ganglion (DRG) neuron and Schwann cell co-culture system as a model of myelination.

Material and Methods

Culture, isolation, and purification of Schwann cells
Animal protocols were reviewed and approved by the Animal Ethics Committee of Nantong University, China (license No. 2014-0001), and the experimental protocol was in accordance with the Guide for the Care and Use of Laboratory Animals (National Institutes of Health Publication, No. 80-23). Precautions were taken to minimize suffering and the number of animals used in each experiment.

Primary cultures of Schwann cells were prepared as previously described (Brockes et al., 1981; Chen et al., 2012). In brief, Schwann cells were harvested from sciatic nerves of 1–3-day-old Sprague-Dawley rats (Experimental Animal Center of Nantong University, Nantong, Jiangsu Province, China, SPF level, no gender requirement). To inhibit fast proliferation of fibroblasts, the Schwann cell purification medium was replaced (**Table 1**) for 1 day, followed by a 1-day recovery period in growth factor-free medium, then refreshed with Schwann cell growth medium. About 7 days later, when the Schwann cell cultures reached confluence, complement-mediated immune cytolysis was performed to eliminate fibroblasts by incubating the cells in 4 μg/mL of anti-Thy-1.1 antibody (Sigma-Aldrich, St. Louis, MO, USA)

for 2 hours on ice and then with 1 mL of rabbit complement (Gibco, Carlsbad, CA, USA) for 1 hour at 37°C. Afterwards, > 98% pure Schwann cells were obtained and the purity was determined by immunocytochemistry.

Culture, isolation, and purification of DRG neurons
DRG neurons were isolated by dissection from embryos of 14.5-day pregnant Sprague-Dawley rats (Experimental Animal Center of Nantong University, Nantong, Jiangsu Province, China. SPF level). One DRG explant was placed into each poly-D-lysine (PDL) (Invitrogen)-coated tissue culture well (24-well dishes, glass cover slips covered with 10 μg/mL PDL before use) along with high-glucose Dulbecco's-modified Eagle's medium (DMEM-HG) (Gibco) containing 10% fetal bovine serum (FBS) (Gibco) and the cells were allowed to adhere for 24 hours. The medium was then replaced with DRG purification medium (**Table 1**) and the non-neuronal cells were eliminated by incubating for 3 days in DRG purification medium. The medium was then replaced with DRG growth medium followed by the addition of purified Schwann cells.

Co-culture of DRG neurons and Schwann cells
The DRG neuron and Schwann cell co-culture system was prepared as previously described (Eldridge et al., 1989). Briefly, purified Schwann cells were co-cultured and growth factors were removed at 4 hours prior to plating on DRG neurons. Then, 0.125% trypsin was used to digest Schwann cells into single cells, and 50,000 Schwann cells were added to each DRG neuron culture coverslip. DRG growth medium was changed 1 day before co-culture, and half of the original medium was discarded after co-culture. A total of 250 μL DMEM-HG containing 10% FBS was added to each well, and the cells were allowed to attach overnight. The DRG neuron and Schwann cell co-cultures were maintained in DRG growth medium for 2 days and then switched to differentiation medium for 4 days. Finally, the co-culture system was maintained in myelination medium to induce myelination. Half of the medium volume was changed every 2 days. After 3–4 days, myelin sheaths were present. In this co-culture process, several specific myelination stages were identified by immunocytochemistry and electron microscopy.

siRNA transfection
Schwann cells were transfected with siRNA using Lipofectamine™ RNAi MAX complexes (Invitrogen) at 4 or 5 days post-purification. ON-TARGET plus Non-targeting control siRNA (catalog D-0018100-01-20, GE Dharmacon, Lafayette, CO, USA) served as the control. The siRNA primer sequences for Rab27a and siRNA Slp2-a are listed in **Table 2**.

Real-time quantitative PCR assay
Total RNAs were extracted using an RNeasy Mini Kit (Qiagen, Hilden, Germany) and cDNA was synthesized using a cDNA Reverse Transcription Kit (Applied Biosystems, Foster, CA, USA). Real-time quantitative PCR was performed using the 7300 Real-Time PCR System (Applied Biosystems). The primers used in this experiment are shown in **Table 3**.

Levels of mRNA were normalized by glyceraldehyde-3-phosphate dehydrogenase (GAPDH) as a reference. All reactions were repeated in triplicate.

Immunocytochemistry

The culture medium was aspirated, and the cells were washed with PBS and then fixed with 4% paraformaldehyde (PFA) for 15 minutes at room temperature and methanol for 10 minutes at −20°C. The non-specific antibody-binding sites were blocked with Immunol Staining Blocking Buffer (Beyotime, Haimen, Jiangsu Province, China) for 1 hour at room temperature, and then the cultures were incubated with primary antibody overnight at 4°C. Antibodies to the following proteins were used at the indicated concentrations: mouse anti-Rab27a (1:100; Abcam, Cambridge, MA, USA), rabbitanti-Slp2-a (1:200; Protein Tech, Chicago, IL, USA), mouse anti-MBP (1:200, Abcam), chicken anti-P0 (1:50; Novus, Littleton, CO, USA), rabbit anti-MAG (1:200; Sigma), and mouse anti-NF (1:600; Sigma). After washing 3 times in PBS to remove excess primary antibody, the cultures were incubated for 1 hour at room temperature with their respective fluorescence-conjugated secondary antibodies (Jackson Immuno Research, West Grove, PA, USA): goat anti-rabbit IgG-Cy3 (H + L), goat anti-mouse IgG-Cy3 (H + L), goat anti-rabbit IgG-Cy5 (H + L), goat anti-mouse IgG-Alexa-488 (H + L), goat anti-rabbit IgG-Alexa-488 (H + L), and goat anti-chicken IgG (H + L) rhodamine, all at a dilution of 1:1,000. After a final PBS washing, the stainings were imaged with a confocal microscope (TCS SP5; Leica Microsystems, Wetzlar, Germany).

Electron microscopy

The co-cultures were examined using electron microscopy at different stages as described (Einheber et al., 1995; Yuan et al., 2004). At the exact stage, the co-culture coverslips were fixed with precooled 2.5% glutaraldehyde (Sigma) and preserved at 4°C.

Scanning electron microscopy

The co-culture cells were washed with tannic acid and then post-fixed with 1% osmium tetraoxide solution (Sigma), dehydrated stepwise twice in increasing concentrations of ethanol and in Tert-butanol, and dried in a critical point drier (Hitachi, Tokyo, Japan). Subsequently, the samples were coated with gold in a JFC-1100 unit (Jeol Inc., Tokyo, Japan) and observed under a scanning electron microscope (JEM-T300, Jeol Inc.).

Transmission electron microscopy

The co-culture coverslips were embedded in 1% agar suitable for obtaining cross-sections of the cultures, post-fixed with 1% osmium tetraoxide solution (Sigma), dehydrated stepwise in increasing concentrations of ethanol, embedded in Epon 812 epoxy resin (Sigma), and cut into transverse sections. Then the ultra-thin transverse sections were stained with lead citrate and uranyl acetate. These sections were examined under a transmission electron microscope (Jeol Inc.).

Western blot assay

Protein was extracted from cultured cells with a buffer containing 1% sodium dodecyl sulfate (SDS, Sigma), 100 mM Tris-HCl, 1 mM phenylmethylsulfonyl fluoride (PMSF, Sigma), and 0.1 mM β-mercaptoethanol (Sigma). After centrifugation at 12,000 r/min for 5 minutes, the supernatant was collected and the protein concentration was determined. Protein extracts were heat denatured at 100°C for 5 minutes, electrophoretically separated on 8% or 12% SDS-PAGE, and transferred to polyvinylidene fluoride (PVDF) membranes (Thermo Fisher Scientific Pierce, Walthan, MA, USA). The membrane was probed with antibodies specific to Rab27a (mouse, 1,000, abcam), Slac2-b (goat, 1:200, SANTA CRUZ Inc., Paso Robles, CA, USA), Slac2-c (rabbit, 1:200, SANTA CRUZ Inc.), Slp2-a (rabbit, 1:800, Protein tech Group, Inc., Chicago, IL, USA), Slp3-a (rabbit, 1:200, Santa Cruz Inc.), Slp4 (rabbit, 1:500, Anbo, San Francisco, CA, USA), MAG (rabbit, 1:800, Sigma), P0 (chicken, 1:800, Novus, Littleton, CO, USA), and PMP22 (rabbit, 1:800, abcam) overnight at 4°C, followed by horseradish peroxidase (HRP)-conjugated secondary antibodies (1:1,000, Beyotime) for 1 hour at room temperature, and detected using the enhanced chemiluminescent substrate kit (ECL, Thermo Fisher Scientific Pierce, Walthan, MA, USA). The image was scanned with a GS800 Densitometer Scanner (Bio-Rad), and the data were analyzed using PDQuest 7.2.0 software (Bio-Rad). β-Actin (mouse, 1:5,000, Sigma) was used as an internal control (Gu et al., 2012; Wang et al., 2012).

Immunoprecipitation

Cultured Schwann cells were lysed in radioimmunoprecipitation assay (RIPA) buffer (Millipore, Billerica, MA, USA) and the lysates were incubated with 10 μg/mL mouse anti-Rab27a antibody (abcam) or mouse IgG control (abcam) on ice overnight with occasional shaking. The antibody-protein complexes were aggregated with Protein G-Agarose (Pierce) overnight on ice, with occasional shaking, and then centrifuged at 8,000 × *g* for 10 minutes. The pellet was washed for elimination of non-specific binding with 1 × RIPA buffer, eluted by 4 × SDS sample buffer without DL-dithiothreitol (DTT), boiled for 10 minutes, and then processed for western blotting.

Statistical analysis

All data are expressed as the mean ± SEM. Differences between two groups were compared using the Student's *t*-test. One-way analysis of variance followed by the Newman-Keuls test was used for the statistical analyses in other tests. The criterion for statistical significance was $P < 0.05$.

Results

Identification of Slp2-a as Rab27a effector in Schwann cells

Complement-mediated cytolysis with anti-Thy-1.1 antibody was used to purify cultured primary Schwann cells to remove contaminating of fibroblasts. To investigate endogenous expression of Rab27 protein family members in Schwann cells, real time-PCR and double staining were used to detect purified Schwann cells. As shown in **Figure 1A–C**,

Table 1 Different culture media for growth, purification, differentiation, and myelination of Schwann cells and dorsal root ganglion (DRG) neurons

	Growth medium	Purification medium	Differentiation medium	Myelination medium
DRGs	Neurobasal medium (NB) (Gibco) containing: 1 × B27 (Invitrogen, Carlsbad, CA, USA) 50 ng/mL nerve growth factor (NGF) (Sigma-Aldrich) 2 mM L-glutamine (Gln) (Sigma-Aldrich) 100 U/mL penicillin/streptomycin (PS) (Invitrogen)	NB containing: 1 × B27 50 ng/mL NGF 10 μM uridine (U) (Sigma-Aldrich) 10 μM 5-fluoro-2'-deoxyuridine (Fdu) (Sigma-Aldrich) 2 mM Gln 100 U/mL PS	High glucose-Dulbecco's modified Eagle's medium (DMEM-HG) (Gibco) containing: 1 × ITS (Sigma-Aldrich) 0.2% bovine serum albumin (BSA) (Sigma-Aldrich) 50 ng/mL NGF 100 U/mL PS	DMEM-HG containing: 15% fetal bovine serum (FBS) (Gibco) 50 μg/mL L-ascorbic acid (AA) (Sigma-Aldrich) 50 ng/mL NGF 100 U/mL PS
Schwann cells	DMEM-HG containing: 10% FBS 2 mM Forskolin (Sigma-Aldrich) 10 ng/mL human heregulin-β1 (HRG) (PeproTech, Rocky Hill, NJ, USA) 100 U/mL PS	DMEM-HG containing: 10% FBS 10 μM cytosine-β-D-arabinofuranoside hydrochloride (Cty-A) (Sigma-Aldrich) 100 U/mL PS		

Table 3 Real time-PCR primers used for Rab27a/b effectors

Rab27a/b and their effectors	Forward primer sequences (5′–3′)	Reverse primer sequences (5′–3′)
Rab27a	TTC CTG CTT CTG TTC GAC CT	TGC TCAC TCG GTG TCT CAA C
Rab27b	CAA CTG CAG GCA AAT GCT TA	TCG ACC TTC CCAG AAT TCA C
Exophilin3-Melanophilin/Slac2-a	GCA TTG ACG GTG GTT CTT TT	GGT CAC GTG GAG GAA ACT GT
Exophilin5-Slac2-b	TGC TGT AGA AAT CGG TGA G	CTG AGT GGG ATG GGA GA
Exophilin8-Myrip/Slac2-c	CCT TGG CTG TTG CCC TAC	GGT CCT ACT CTT CGG CTT GG
Exophilin7-Sytl1/Slp1	GAC CAG GAC CTG AAG CTG AG	GGA CGA GGT CAG AAC CAA AA
Exophilin4-Sytl2/Slp2-a	ATG AGT GGC AGT GTG ATG AGC GTT	TCA CTT GGA AAG CTT GGC AAT
Exophilin6-Sytl3/Slp3-a	AGA ACA CTC TGG ACC CGA CTT	CGC CTT GGG CTT CAC CT
Exophilin2-Granuphilin/Sytl4/Slp4	GCG AGT GGG TGG TTT CAT	CAG TCA GTT CCA GGC ACA T
Exophilin9-Sylt5/Slp5	CAA AAC CAA GAG CAA GCA CA	AGC CAG AGA CCG ACT TGA AA
Exophilin1-Rabphilin 3a	GTC AAG CTC TGG CTG AAA CC	GCA GCC TCC GAT GTA ATC AT
Noc2	CCC CTG TGG CTG TGT AAG AT	TCT GAG GCT GTG GTT CTG TG
Munc13-4	GCG GAA ACC ACT TCT GAG AG	CCA GCT CAG GGA ATT CAT GT

Table 2 siRNA primer sequences for Rab27a and siRNA Slp2-a

Primer	Sequences (5′–3′)
Rat-Rab27a-siRNA	Sense: AGA CTC TGG AGT GGG GAA GdTdT Antisense: UCU GAG ACC UCA CCC CUU CdTdT
Rat-Slp2-a-siRNA-1#	Sense: CUG GGA CCA UUA UAA ACU AdTdT Antisense: UAG UUU AUA AUG GUC CCA GdTdT
Rat-Slp2-a-siRNA-2#	Sense: GGG AUA CGU UUA AGC GCA AdTdT Antisense: UUG CGC UUA AAC GUA UCC CdTdT
Rat-Slp2-a-siRNA-3#	Sense: GGC AUC GGG AUA CGU UUA AdTdT Antisense: UAG UUU AUA AUG GUC CCA GdTdT

Schwann cells only expressed Rab27a protein, although real time-PCR results also showed weak Rab27b expression. Results are consistent with previous reports that Rab27a is primarily expressed outside the CNS and Rab27b is expressed in the central nervous system (Izumi, 2007). To identify the Rab27a effectors in Schwann cells, we analyzed mRNA expression of 11 different Rab27a/b effectors in Schwann cells according to a previous study (Izumi, 2007). As shown in **Figure 1D**, expressions of Slac2-b, Slac2-c, Slp2-a, Slp3-a, and Slp4 mRNA were readily visualized in Schwann cells. Western blotting identified high expression of only Slp2-a in Schwann cells (**Figure 1E**). Double Slp2-a and Rab27a immunostaining revealed co-localization of Slp2-a with Rab27a in cultured Schwann cells (**Figure 1F**). Additionally, co-immunoprecipitation experiments clearly showed an interaction between Slp2-a and Rab27a in cultured Schwann cells (**Figure 1G**). These results suggested that Slp2-a is endogenously expressed as a Rab27a effector in Schwann cells.

Myelination model of DRG neurons co-cultured with Schwann cells

To examine the role of Rab27a and Slp2-a in Schwann cells on myelin formation *in vitro*, we established a myelination model of DRG neurons co-cultured with Schwann cells. Previous groups have successfully used this model to study PNS myelination (Johnson et al., 2001; Liu et al., 2005; Court et al., 2011). As shown in **Figure 2**, about 2 weeks after Schwann cells were added to the pure DRG neuron cultures, phase-contrast and fluorescence microscopy revealed myelin sheaths in the co-culture. Myelin sheaths were identifiable by the segregation structure in compact myelin sheaths under phase-contrast microscopy observation (**Figure 2A**) and the segregation of MAG-positive signals
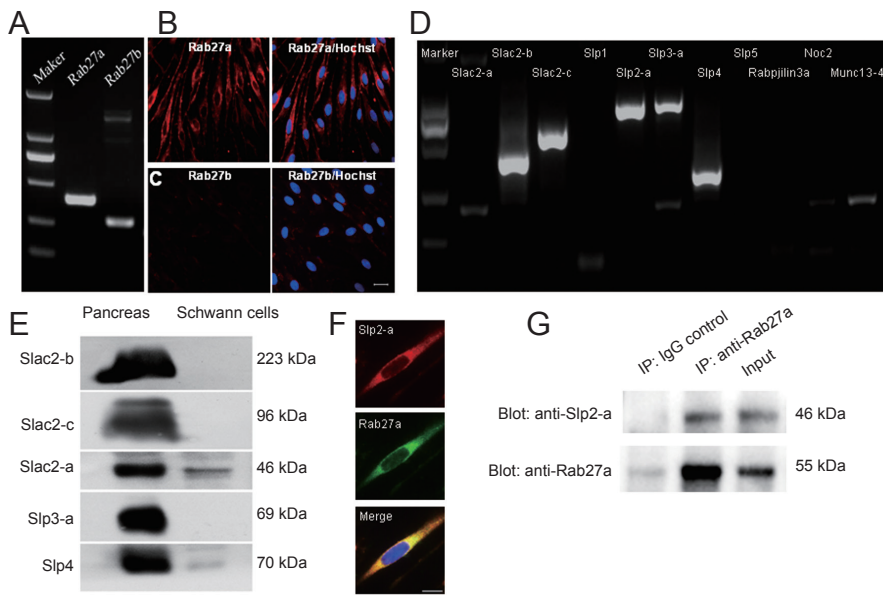
Figure 1 Identification of Slp2-a as a Rab27a effector in cultured Schwann cells.

(A) Real-time PCR results show *Rab27a* (399 bp) and *Rab27b* (275 bp) mRNA expression in cultured pure Schwann cells. (B, C) Double-staining of Rab27a or Rab27b and Hoechst shows that cultured Schwann cells only express Rab27a protein. Scale bar: 20 μm. (D) RT-PCR results show mRNA levels of eleven Rab27a/b effectors in cultured Schwann cells. Eleven Rab27a/b effectors, including *Slac2-b* (407 bp), *Slac2-c* (566 bp), *Slp2-a* (713 bp), *Slp3-a* (744 bp), and *Slp4* (312 bp) are readily visualized. (E) Western blotting results show high expression of only Slp2-a was in cultured Schwann cells. (F) Triple immunostaining of Slp2-a, Rab27a, and Hoechst reveals co-localization of Slp2-a with Rab27a in cultured Schwann cells. Scale bar: 10 μm. (G) Co-immunoprecipitation experiments show that Slp2-a interacts with Rab27a in cultured Schwann cells.
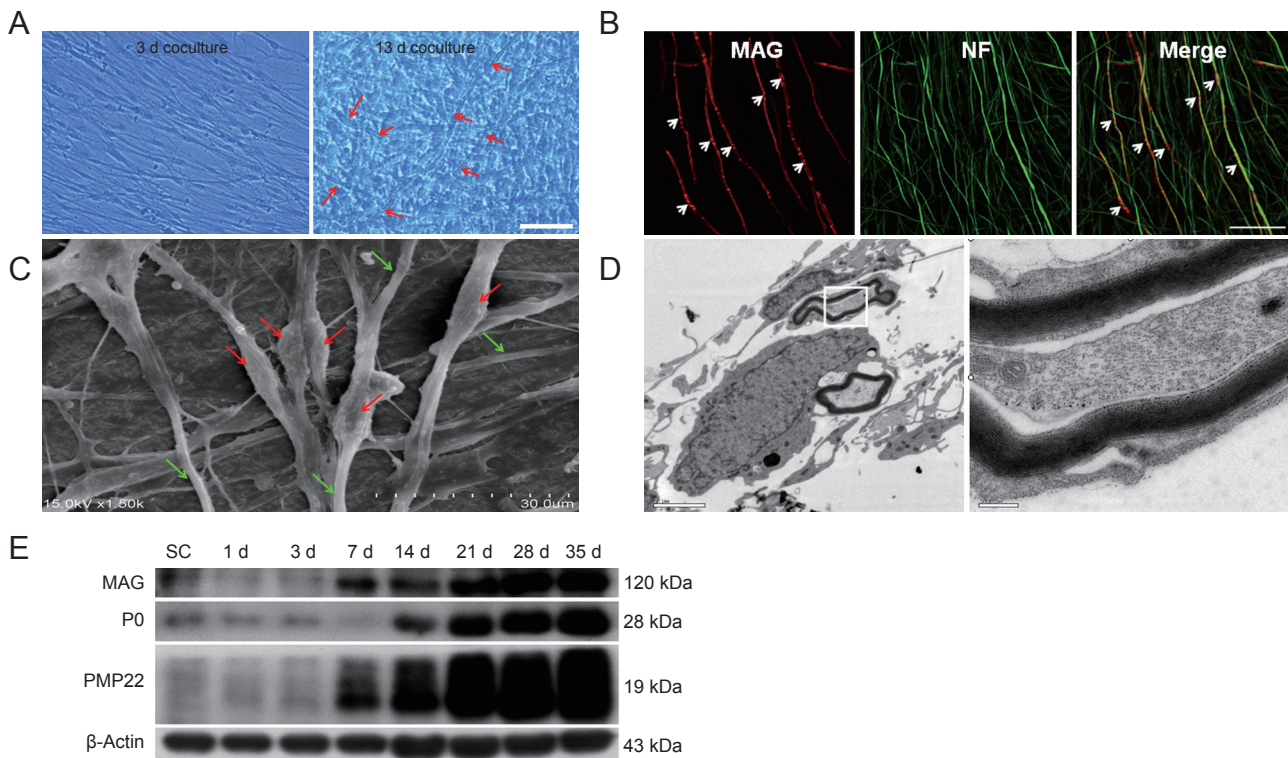

Figure 2 Establishing a myelination model of DRG neurons co-cultured with Schwann cells.

(A) Phase-contrast microscopy at 3 and 13 days after the establishment of a DRG neuron and Schwann cell co-culture. Arrows indicate myelin sheath-like structures. Scale bar: 50 μm. (B) Double-staining with anti-MAG (red) and anti-NF (green) to examine myelination. Arrows indicate segregation of MAG staining in the neurites of DRG neurons. Scale bar: 50 μm. (C) Scanning electron microscopy shows Schwann cells surrounding DRG neuron neurites and the formation of myelin segments. The diameters of the myelinated axons are thicker (red arrows) than the neuritis of DRG neurons (green arrows). Scale bar: 30 μm. (D) Transmission electron microscopy also shows the typical compact myelin structure. Right: High-magnification image from inset box. Scale bar: 2 μm on the left and 0.2 μm on the right. (E) Western blot images of expression of myelin proteins MAG, P0, and PMP22 at 1, 3, 7, 14, 21, 28 and 35 days after co-culture. β-Actin served as a protein loading control. Compared with purified Schwann cells alone, the DRG neuron and Schwann cell co-cultures induce a significant increase in all myelin proteins. DRG: Dorsal root ganglion; d: days.
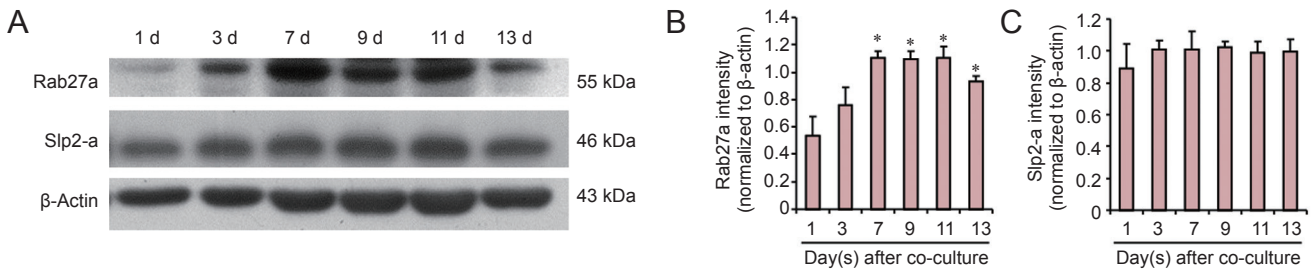
Figure 3 DRG neurons co-cultured with Schwann cells induce persistent up-regulation of Rab27a in Schwann cells.
(A) Rab27a and Slp2-a expression in Schwann cells, as shown by western blotting, at 1, 3, 7, 9, 11, and 13 days after co-culture. (B, C) Quantification of Rab27a and Slp2-a expression in Schwann cells at 1, 3, 7, 9, 11, and 13 days after co-culture as detected by western blot assay. Optical density results are presented as a fold of β-actin expression. All data are expressed as the mean ± SEM, with n = 4 cultures/group. Differences between groups were analyzed by one-way analysis of variance followed by the Newman-Keuls test. *P < 0.05, vs. co-culture at 1 day. d: Days.
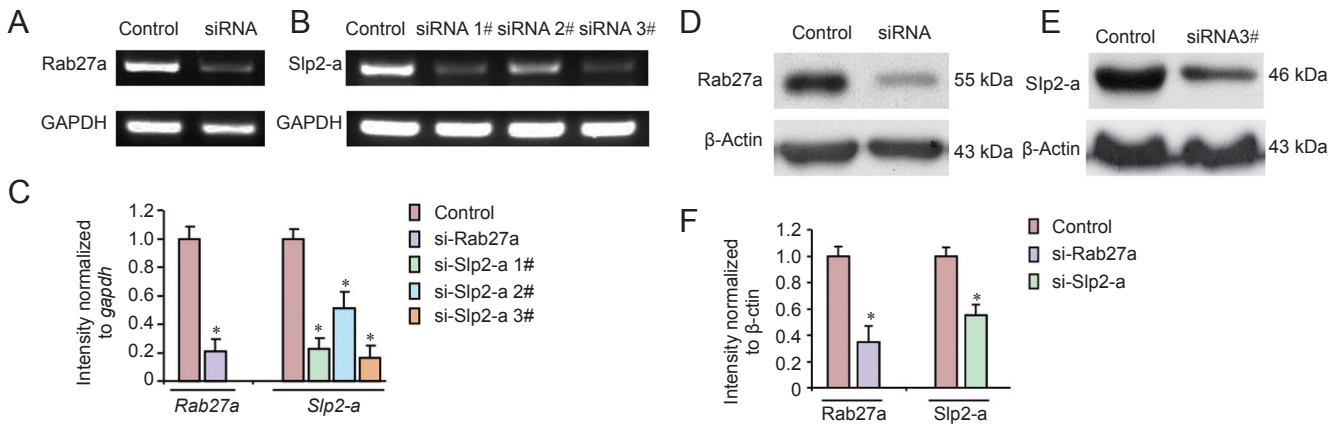

Figure 4 Rab27a and Slp2-a siRNA reduces Rab27a and Slp2-a expressions in cultured Schwann cells.
(A, B) Schwann cells were transfected with (A) siRNA-$Rab27a$ and (B) three different sequences of siRNA-$Slp2$-a. mRNA levels of $Rab27a$ and $Slp2$-a are significantly reduced following respective siRNA transfections. (C) Quantification of $Rab27a$ and $Slp2$-a mRNA levels in transfected Schwann cells was detected by western blot assay. Optical density results are presented as a fold of $Gapdh$ expression. (D, E) Schwann cells were transfected with (D) siRNA-$Rab27a$ and (E) siRNA-$Slp2$-a sequence #3. Each siRNA dramatically reduces expression of their respective target genes. (F) Quantification of Rab27a and Slp2-a protein levels in siRNA-transfected Schwann cells by western blot assay. Optical density results are presented as a fold of β-actin expression. Data are presented as the mean ± SEM. Student's t-test, n = 3 cultures/group. *P < 0.05, vs. control group.
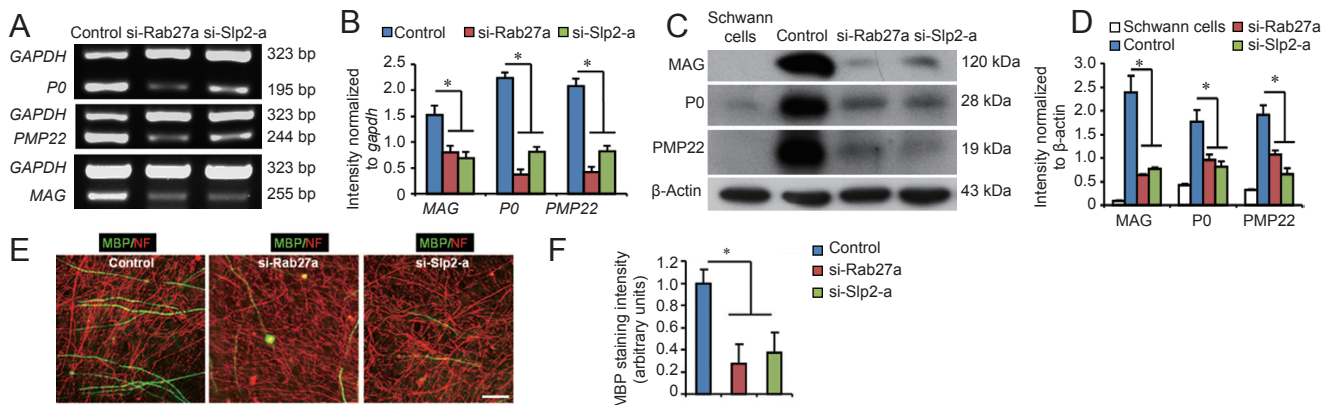

Figure 5 Knockdown of Rab27a and Slp2-a in Schwann cells reduces myelin protein expression and myelin-like membrane formation in the DRG neuron and Schwann cell co-cultures.
(A–D) Compared with the non-targeting control siRNA, Rab27a and Slp2-a knockdown in the purified Schwann cells prior to seeding with DRG neurons significantly reduces mRNA levels (A) and protein expression (C) of myelin proteins MAG, P0, and PMP22 at 14 days after co-culture. Optical density results are presented as a fold of $gapdh$ expression (B) and actin expression (D). (E) Double-immunostaining of MBP and NF in different groups at 14 days in co-culture also shows that silencing of Rab27a and Slp2-a reduces the formation of MAG-positive myelin-like membranes. Scale bar: 50 μm. (F) Quantification of MBP immunofluorescence intensity in different groups at 14 days after co-culture. Student's t-test, n = 3 cultures/group. All data represent mean ± SEM. *P < 0.05 (one-way analysis of variance followed by the Newman-Keuls test). DRG: Dorsal root ganglion; MAG: myelin associated glycoprotein; NF: neurofilament; PMP22: peripheral myelin protein 22; MBP: myelin basic protein; P0: protein zero; GAPDH: glyceraldehyde-3-phosphate dehydrogenase.

by immunostaining (**Figure 2B**). Scanning electron microscopy (**Figure 2C**) revealed that Schwann cells surrounded the DRG neuronneurites and formed myelin segments, with a diameter longer than that of unmyelinated neurites. Transmission electron microscopy also showed the typical compact myelin structure (**Figure 2D**). Myelin protein expressions, including MAG, P0, and PMP22, were detected by western blotting at 1, 3, 7, 14, 21, 28, and 35 days after co-culture. Compared with purified Schwann cells, the DRG neuron and Schwann cell co-culture resulted in increased expression of all myelin proteins, which peaked at 35 days (**Figure 2E**). These results showed that a stable and reliable *in vitro* myelination model was established.

Silencing of Rab27a and Slp2-a in the DRG neuron and Schwann cell co-culture reduces myelin protein expression and impairs formation of myelin-like membranes

Using the DRG neuron and Schwann cell co-culture myelination model, we examined expression of Rab27a and Slp2-a at different time points following co-culture. As shown in **Figure 3**, western blot results showed significantly increased Rab27a expression at 3 days, which peaked at 7 days and remained increased at 13 days. However, Slp2-a expression remained unchanged after co-culture.

Next, siRNA silencing of Rab27a and Slp2-a was used in Schwann cells to examine the roles of Rab27a and Slp2-a in myelination. First, the gene silencing efficiency of siRNA was detected using the same sequence of siRNA-Rab27a as our previous report (Chen et al., 2012), as well as three different siRNA-Slp2-a sequences. Gene silencing efficiency was then compared by real-time quantitative PCR. As shown in **Figure 4A–C**, siRNA dramatically reduced Rab27a and Slp2-a levels in Schwann cells. Among the three different sequences of Slp2-a siRNA, sequence #3 exhibited the strongest effect. Expressions of Rab27a and Slp2-a protein were analyzed in Schwann cells by western blotting. As shown in **Figure 4D–F**, Rab27a and Slp2-a protein expressions were dramatically reduced.

Finally, purified Schwann cells were transfected with siRNA prior to seeding with DRG neurons, and then myelin protein mRNA levels and protein expressions were determined. As shown in **Figure 5A–D**, compared with the control group, Rab27a and Slp2-a knockdown significantly reduced both mRNA levels and protein expression of MAG, P0, and PMP22 after 14 days in co-culture. Furthermore, MBP immunostaining after 14 days of co-culture also showed that Rab27a or Slp2-a silencing impaired the formation of myelin-like membranes (**Figure 5E**, **F**). These results suggest that the Rab27a-Slp2-a complex plays an important role in Schwann cell myelination, especially in the early stage.

Discussion

The onset and maintenance of myelination in the PNS depends on myelin protein synthesis and transport (Salzer, 2015; Kondo and Duncan, 2016; Schulz et al., 2016; Taveggia, 2016). Our previous results indicate that Rab27a regulates lysosomal exocytosis and is involved in myelin

protein trafficking in Schwann cells (Chen et al., 2012). This study aimed to identify the signals associated with Rab27a in Schwann cells. Our results demonstrated the importance of the Rab27a/Slp2-a complex in Schwann cell myelination. The underlying mechanism was determined through multiple experimental approaches, showing 1) Slp2-a was endogenously expressed as a Rab27a effector in Schwann cells; 2) the *in vitro* Schwann cell myelination model was established in our experiment; 3) Rab27a expression was significantly increased during Schwann cell myelination; 4) silencing of Rab27a and Slp2-a in Schwann cells not only reduced myelin protein expression, but also impaired the formation of myelin-like membranes in DRG neuron and Schwann cell co-cultures.

Rab27a is associated with secretory lysosomes and intracellular protein trafficking (Blott and Griffiths, 2002; Izumi, 2007; Johnson et al., 2013; Catz, 2014; Ishida et al., 2014; Chen et al., 2015; Feng et al., 2016). It has been proposed that Rab27a regulates different membrane transport events by interacting with a different set of specific effectors (Li et al., 2014; Yasuda and Fukuda, 2014; Yamaoka et al., 2015a, 2016; Yasuda et al., 2015; Jiang et al., 2016; Kowluru, 2016; Netter et al., 2016). Three groups of Rab27a effectors from a total of 11 Rab27a/b effectors, including synaptotagmin-like protein (Slp), Slp homologue lacking C2 domains (Slac2), and Munc13-4, have been identified in mice and humans (Fukuda, 2005, 2013; Izumi, 2007; Ishida et al., 2014; Jiang et al., 2016; Kowluru, 2016; Netter et al., 2016). Results from the present study showed that Slp2-a and its binding effector Rab27a form a complex in Schwann cells. In general, Slp2-a can promote docking of Rab27a-containing vesicles to the plasma membrane in certain types of secretory cells (Kuroda and Fukuda, 2004; Saegusa et al., 2006; Holt et al., 2008; Ménasché et al., 2008; Fukuda, 2013; Yasuda and Fukuda, 2014; Yasuda et al., 2015). Although the Rab27a effector function of Slp2-a has been well established, the role of Slp2-a in myelination remains poorly understood. Results from the present study showed that Slp2-a silencing in Schwann cells not only reduced myelin protein expression, but also impaired formation of myelin-like membranes in the DRG neuron and Schwann cell co-cultures. The mechanisms responsible for decreased myelin protein expression by Rab27a and Slp2-a knockdown are not clear, but could be due to negative feedback of myelination.

The *in vitro* model of rat DRG explant and Schwann cell co-cultures has been used in various studies (Johnson et al., 2001; Liu et al., 2005; Court et al., 2011; Liu and Chan, 2016) to determine the intrinsic molecular mechanisms responsible for myelination, including the complex regulation of transcription factors and myelin protein during myelin formation (Pereira et al., 2012; Salzer, 2015). In this study, we established a stable and reliable *in vitro* myelination model and transmission electron microscopy images confirmed the typical compact myelin structure. We also analyzed expression of several myelin proteins in this model using western blot analysis at different time points.

Above all, this is the first demonstration that the Rab27a/

Slp2-a complex affects Schwann cell myelination *in vitro*. These findings show an interesting link between myelin biogenesis and lysosome-related organelle exocytosis, providing a basis for clinical treatments of demyelinating diseases.

References

Blott EJ, Griffiths GM (2002) Secretory lysosomes. Nat Rev Mol Cell Biol 3:122-131.

Brockes JP, Fryxell KJ, Lemke GE (1981) Studies on cultured Schwann cells: the induction of myelin synthesis, and the control of their proliferation by a new growth factor. J Exp Biol 95:215-230.

Catz SD (2014) The role of Rab27a in the regulation of neutrophil function. Cell Microbiol 16:1301-1310.

Chen G, Zhang Z, Wei Z, Cheng Q, Li X, Li W, Duan S, Gu X (2012) Lysosomal exocytosis in Schwann cells contributes to axon remyelination. Glia 60:295-305.

Chen TC, Hsieh CH, Sarnow P (2015) Supporting Role for GTPase Rab27a in Hepatitis C Virus RNA Replication through a Novel miR-122-Mediated Effect. PLoS Path 11:e1005116.

Court FA, Zambroni D, Pavoni E, Colombelli C, Baragli C, Figlia G, Sorokin L, Ching W, Salzer JL, Wrabetz L, Feltri ML (2011) MMP2–9 cleavage of dystroglycan alters the size and molecular composition of Schwann cell domains. J Neurosci 31:12208-12217.

da Silva TF, Eira J, Lopes AT, Malheiro AR, Sousa V, Luoma A, Avila RL, Wanders RJA, Just WW, Kirschner DA, Sousa MM, Brites P (2014) Peripheral nervous system plasmalogens regulate Schwann cell differentiation and myelination. J Clin Invest 124:2560-2570.

de Duve C (2005) The lysosome turns fifty. Nat Cell Biol 7:847-849.

Domènech-Estévez E, Baloui H, Repond C, Rosafio K, Médard JJ, Tricaud N, Pellerin L, Chrast R (2015) Distribution of monocarboxylate transporters in the peripheral nervous system suggests putative roles in lactate shuttling and myelination. J Neurosci 35:4151-4156.

Duncan LE, Holmans PA, Lee PH, O'Dushlaine CT, Kirby AW, Smoller JW, Öngür D, Cohen BM (2014) Pathway analyses implicate glial cells in schizophrenia. PLoS One 9:e89441.

Einheber S, Hannocks MJ, Metz CN, Rifkin DB, Salzer JL (1995) Transforming growth factor-beta 1 regulates axon/Schwann cell interactions. J Cell Biol 129:443-458.

Eldridge CF, Bunge MB, Bunge RP (1989) Differentiation of axon-related Schwann cells in vitro: II. Control of myelin formation by basal lamina. J Neurosci 9:625-638.

Faust PL, Kaye EM, Powers JM (2010) Myelin lesions associated with lysosomal and peroxisomal disorders. Expert Rev Neurother 10:1449-1466.

Feldmann A, Amphornrat J, Schönherr M, Winterstein C, Möbius W, Ruhwedel T, Danglot L, Nave KA, Galli T, Bruns D, Trotter J, Krämer-Albers EM (2011) Transport of the major myelin proteolipid protein is directed by VAMP3 and VAMP7. J Neurosci 31:5659-5672.

Feng F, Jiang Y, Lu H, Lu X, Wang S, Wang L, Wei M, Lu W, Du Z, Ye Z, Yang G, Yuan F, Ma Y, Lei X, Lu Z (2016) Rab27A mediated by NF-κB promotes the stemness of colon cancer cells via up-regulation of cytokine secretion. Oncotarget doi: 10.18632/oncotarget.11454.

Fukuda M (2005) Versatile role of Rab27 in membrane trafficking: focus on the Rab27 effector families. J Biochem 137:9-16.

Fukuda M (2013) Rab27 effectors, pleiotropic regulators in secretory pathways. Traffic 14:949-963.

Gökbuget D, Pereira JA, Bachofner S, Marchais A, Ciaudo C, Stoffel M, Schulte JH, Suter U (2015) The Lin28/let-7 axis is critical for myelination in the peripheral nervous system. Nat Commun 6:8584.

Gonzalez S, Berthelot J, Jiner J, Perrin-Tricaud C, Fernando R, Chrast R, Lenaers G, Tricaud N (2016) Blocking mitochondrial calcium release in Schwann cells prevents demyelinating neuropathies. J Clin Invest 126:2773.

Gu Y, Ji Y, Zhao Y, Liu Y, Ding F, Gu X, Yang Y (2012) The influence of substrate stiffness on the behavior and functions of Schwann cells in culture. Biomaterials 33:6672-6681.

Heller BA, Ghidinelli M, Voelkl J, Einheber S, Smith R, Grund E, Morahan G, Chandler D, Kalaydjieva L, Giancotti F, King RH, Fejes-Toth AN, Fejes-Toth G, Feltri ML, Lang F, Salzer JL (2014) Functionally distinct PI 3-kinase pathways regulate myelination in the peripheral nervous system. J Cell Biol 204:1219-1236.

Holt O, Kanno E, Bossi G, Booth S, Daniele T, Santoro A, Arico M, Saegusa C, Fukuda M, Griffiths GM (2008) Slp1 and Slp2-a localize to the plasma membrane of CTL and contribute to secretion from the immunological synapse. Traffic 9:446-457.

Hou Y, Ernst SA, Stuenkel EL, Lentz SI, Williams JA (2015) Rab27A Is Present in Mouse Pancreatic Acinar Cells and Is Required for Digestive Enzyme Secretion. PLoS One 10:e0125596.

Ishida M, Arai SP, Ohbayashi N, Fukuda M (2014) The GTPase-deficient Rab27A(Q78L) mutant inhibits melanosome transport in melanocytes through trapping of Rab27A effector protein Slac2-a/melanophilin in their cytosol: development of a novel melanosome-targetinG tag. J Biol Chem 289:11059-11067.

Izumi T (2007) Physiological roles of Rab27 effectors in regulated exocytosis. Endocr J 54:649-657.

Jiang S, Shen D, Jia WJ, Han X, Shen N, Tao W, Gao X, Xue B, Li CJ (2016) GGPPS-mediated Rab27A geranylgeranylation regulates β cell dysfunction during type 2 diabetes development by affecting insulin granule docked pool formation. J Pathol 238:109-119.

Johnson JL, Napolitano G, Monfregola J, Rocca CJ, Cherqui S, Catz SD (2013) Upregulation of the Rab27a-dependent trafficking and secretory mechanisms improves lysosomal transport, alleviates endoplasmic reticulum stress, and reduces lysosome overload in cystinosis. Mol Cell Biol 33:2950-2962.

Johnson MI, Bunge RP, Wood PM (2001) Primary Cell Cultures for the Study of Myelination. In: Protocols for Neural Cell Culture (Fedoroff S, Richardson A, eds), pp 95: Humana Press.

Kim JD, Willetts L, Ochkur S, Srivastava N, Hamburg R, Shayeganpour A, Seabra MC, Lee JJ, Moqbel R, Lacy P (2013) An essential role for Rab27a GTPase in eosinophil exocytosis. J Leukocyte Biol 94:1265-1274.

Klein D, Martini R (2016) Myelin and macrophages in the PNS: An intimate relationship in trauma and disease. Brain Res 1641(Pt A):130-138.

Kondo Y, Duncan ID (2016) Myelin repair by transplantation of myelin-forming cells in globoid cell leukodystrophy. J Neurosci Res 94:1195-1202.

Kowluru A (2016) A lack of 'glue' misplaces Rab27A to cause islet dysfunction in diabetes. J Pathol 238:375-377.

Kuroda TS, Fukuda M (2004) Rab27A-binding protein Slp2-a is required for peripheral melanosome distribution and elongated cell shape in melanocytes. Nat Cell Biol 6:1195-1203.

Kwon HS, Johnson TV, Joe MK, Abu-Asab M, Zhang J, Chan CC, Tomarev SI (2013) Myocilin mediates myelination in the peripheral nervous system through ErbB2/3 signaling. J Biol Chem 288:26357-26371.

Li W, Hu Y, Jiang T, Han Y, Han G, Chen J, Li X (2014) Rab27 regulates exosome secretion from lung adenocarcinoma cells A549: involvement of EPI64. APMIS 122:1080-1087.

Liu C, Chan C (2016) An approach to enhance alignment and myelination of dorsal root ganglion neurons. J Vis Exp doi: 10.3791/54085.

Liu N, Varma S, Shooter EM, Tolwani RJ (2005) Enhancement of Schwann cell myelin formation by K252a in the Trembler-J mouse dorsal root ganglion explant culture. J Neurosci Res 79:310-317.

Luo S, Jaegle M, Li R, Ehring GR, Meijer D, Levinson SR (2014) The sodium channel isoform transition at developing nodes of ranvier in the peripheral nervous system: Dependence on a Genetic program and myelination-induced cluster formation. J Comp Neurol 522:4057-4073.

Ménasché G, Ménager MM, Lefebvre JM, Deutsch E, Athman R, Lambert N, Mahlaoui N, Court M, Garin J, Fischer A, de Saint Basile G (2008) A newly identified isoform of Slp2a associates with Rab27a in cytotoxic T cells and participates to cytotoxic granule secretion. Blood 112:5052-5062.

Ma KH, Hung HA, Svaren J (2016) Epigenomic Regulation of Schwann Cell Reprogramming in Peripheral Nerve Injury. J Neurosci 36:9135-9147.

Marsden D, Levy H (2010) Newborn screening of lysosomal storage disorders. Clin Chem 56:1071-1079.

Miyamoto Y, Tamano M, Torii T, Kawahara K, Nakamura K, Tanoue A, Takada S, Yamauchi J (2016) Data supporting the role of Fyn in initiating myelination in the peripheral nervous system. Data Brief 7:1098-1105.

Montani L, Buerki-Thurnherr T, de Faria JP, Pereira JA, Dias NG, Fernandes R, Gonçalves AF, Braun A, Benninger Y, Böttcher RT, Costell M, Nave K-A, Franklin RJM, Meijer D, Suter U, Relvas JB (2014) Profilin 1 is required for peripheral nervous system myelination. Development 141:1553-1561.

Nave KA, Werner HB (2014) Myelination of the nervous system: mechanisms and functions. Annu Rev Cell Dev Biol 30:503-533.

Netter P, Chan SK, Banerjee PP, Monaco-Shawver L, Noroski LM, Hanson IC, Forbes LR, Mace EM, Chinen J, Gaspar HB, Sleiman P, Hakonarson H, Klein C, Ehlayel MS, Orange JS (2016) A novel Rab27a mutation binds melanophilin, but not Munc13-4, causing immunodeficiency without albinism. J Allergy Clin Immunol 138:599-601.e3.

Pereira JA, Lebrun-Julien F, Suter U (2012) Molecular mechanisms regulating myelination in the peripheral nervous system. Trends Neurosci 35:123-134.

Prolo LM, Vogel H, Reimer RJ (2009) The lysosomal sialic acid transporter sialin is required for normal CNS myelination. J Neurosci 29:15355-15365.

Rao SN, Pearse DD (2016) Regulating axonal responses to injury: the intersection between signaling pathways involved in axon myelination and the inhibition of axon regeneration. Front Mol Neurosci 9:33.

Saegusa C, Tanaka T, Tani S, Itohara S, Mikoshiba K, Fukuda M (2006) Decreased basal mucus secretion by Slp2-a-deficient gastric surface mucous cells. Genes Cells 11:623-631.

Salzer JL (2015) Schwann cell myelination. Cold Spring Harb Perspect Biol 7:a020529.

Schulz A, Büttner R, Hagel C, Baader SL, Kluwe L, Salamon J, Mautner VF, Mindos T, Parkinson DB, Gehlhausen JR, Clapp DW, Morrison H (2016) The importance of nerve microenvironment for schwannoma development. Acta Neuropathol 132:289-307.

Shen YT, Gu Y, Su WF, Zhong JF, Jin ZH, Gu XS, Chen G (2016) Rab27b is Involved in Lysosomal Exocytosis and Proteolipid Protein Trafficking in Oligodendrocytes. Neurosci Bull 32:331-340.

Shimada-Sugawara M, Sakai E, Okamoto K, Fukuda M, Izumi T, Yoshida N, Tsukuba T (2015) Rab27A regulates transport of cell surface receptors modulating multinucleation and lysosome-related organelles in osteoclasts. Sci Rep 5:9620.

Taveggia C (2016) Schwann cells–axon interaction in myelination. Curr Opin Neurobiol 39:24-29.

Trajkovic K, Dhaunchak AS, Goncalves JT, Wenzel D, Schneider A, Bunt G, Nave KA, Simons M (2006) Neuron to glia signaling triggers myelin membrane exocytosis from endosomal storage sites. J Cell Biol 172:937-948.

Wang Y, Tang X, Yu B, Gu Y, Yuan Y, Yao D, Ding F, Gu X (2012) Gene network revealed involvements of Birc2, Birc3 and Tnfrsf1a in anti-apoptosis of injured peripheral nerves. PLoS One 7:e43436.

White R, Krämer-Albers E-M (2014) Axon-glia interaction and membrane traffic in myelin formation. Front Cell Neurosci 7:284.

Yamaoka M, Ishizaki T, Kimura T (2015a) Interplay between Rab27a effectors in pancreatic β-cells. World J Diabetes 6:508-516.

Yamaoka M, Ishizaki T, Kimura T (2015b) GTP- and GDP-dependent rab27a effectors in pancreatic beta-cells. Biol Pharm Bull 38:663-668.

Yamaoka M, Ando T, Terabayashi T, Okamoto M, Takei M, Nishioka T, Kaibuchi K, Matsunaga K, Ishizaki R, Izumi T, Niki I, Ishizaki T, Kimura T (2016) PI3K regulates endocytosis after insulin secretion by mediating signaling crosstalk between Arf6 and Rab27a. J Cell Sci 129:637-649.

Yasuda T, Fukuda M (2014) Slp2-a controls renal epithelial cell size through regulation of Rap-ezrin signaling independently of Rab27. J Cell Sci 127:557-570.

Yasuda T, S. Mrozowska P, Fukuda M (2015) Functional analysis of Rab27A and its effector Slp2-a in renal epithelial cells. Methods Mol Biol 1298:127-139.

Yuan Y, Zhang P, Yang Y, Wang X, Gu X (2004) The interaction of Schwann cells with chitosan membranes and fibers in vitro. Biomaterials 25:4273-4278.

Zhang Z, Chen G, Zhou W, Song A, Xu T, Luo Q, Wang W, Gu XS, Duan S (2007) Regulated ATP release from astrocytes through lysosome exocytosis. Nat Cell Biol 9:945-953.

Copyedited by Copper C, Norman C, Su WF, Yu J, Li CH, Li JY, Song LP, Zhao M